Direct Evidence of Multifractal Atmospheric Cascades from Planetary Scales down to 1 km

S. Lovejoy,[1] D. Schertzer,[2] and J. D. Stanway[1]
[1]*Physics Department, McGill University, Montreal, Canada*
[2]*L.M.M., P. M. Curie University and CNRS, Paris, France*
(Received 6 July 2000; revised manuscript received 20 February 2001)

We use 909 satellite images spanning the scale range 1–5000 km at both visible and infrared wavelengths to show that the variability at all observed scales and at all levels of intensity is very close to that predicted for a direct multiplicative scale invariant cascade starting at planetary scales. To within 1.6%/octave in scale, the observed type of (multi)scaling is very close to that theoretically predicted for universal multifractals, including multifractal phase transitions. Because of the strong vertical stratification, the scaling cannot be isotropic; these findings thus give strong support to the anisotropic "unified scaling" model of atmospheric dynamics.

DOI: 10.1103/PhysRevLett.86.5200 PACS numbers: 92.60.Ek, 47.27.–i, 47.53.+n, 92.70.Cp

In his seminal book [1], Richardson suggested that atmospheric dynamics were ruled by a cascade of energy injected by solar forcing at the largest scales cascading scale after scale until finally dissipated. Unfortunately, due to the theoretical focus on (local) isotropic theories of turbulence — first in three dimensions (leading to the famous $k^{-5/3}$ Kolmogorov law [2]) and then in two dimensions (where it led to small scale k^{-3} and large scale $k^{-5/3}$ laws [3,4]), atmospheric turbulence was circumscribed to regimes with relatively modest scale ratios. In spite of the strong anisotropy due to gravity and the Coriolis force the focus is still on the isotropic special cases which at best can apply only over scale ranges much smaller or much larger than the scale thickness of the mean pressure (roughly 10 km).

The 3D/2D "dimensional transition" at around 10 km was called the "mesoscale gap" and was initially given some empirical support by estimates of wind spectra [5,6]. In spite of strong criticism [7,8] it was eventually consecrated in Monin's [9] influential work. However, developments in the 1980s seriously undermined this picture and led to a renewed interest in cascades. On the empirical side, the first large scale campaign specifically to measure the horizontal velocity spectrum (the GASP experiment [10,11]) failed to find evidence of a mesoscale spectral gap anywhere near 10 km; instead it found $k^{-5/3}$ behavior extending to hundreds of kilometers; this was consistent with analyses of cloud "perimeters" which showed excellent scaling over the range 1–1000 km [12], as well as the consistent empirical evidence from the 1960s onwards [13–17] that the vertical spectrum of the horizontal wind follows Bogliano-Obhukhov $k^{-11/5}$ scaling throughout the troposphere.

In the 1980s, it became clear that cascades were generic multifractal processes. The notion of scale invariance itself was formulated as a rather general, but nonclassical, symmetry principle [13] in which isotropy ("self-similarity") was neither required nor expected. It was hence more logical to postulate a scaling but anisotropic cascade rather than separate small and large scale isotropic cascades (the "unified scaling model of the atmosphere" [17,18]). This "generalized scale invariance" implies anisotropic cascades in which the effects of anisotropy (differential stretching, rotation, compression, etc.), yield structures whose appearance systematically changes with scale. Phenomenological classifications based on morphologies are misleading and could conceal a common cascade dynamics. Indeed, Refs. [19,20] showed — in spite of appearances to the contrary — that classical phenomenological space-time ("Stommel") diagrams of the atmosphere actually imply a scaling velocity which varies with scale according to the Kolmogorov law over the entire range of meteorologically significant scales.

Most tests of the extent and type of atmospheric scaling have concentrated on the velocity field (e.g., [21,22]) with the result that there is now agreement that at least at the small scales, it is indeed multifractal as predicted by cascade theories; the debate (see [23]) is now primarily on the exact type of cascade. Unfortunately, due to the strong intermittency it is very difficult to get adequate statistics. Recently, the situation has clarified somewhat due to spectral analyses of aircraft wind data in the troposphere [24] and stratosphere [25] (see also [26]). Out to about 500 km there is agreement that the spectrum is roughly $k^{-5/3}$; however, at larger scales, the stratospheric spectrum continues as $k^{-5/3}$ out to at least 3000 km, whereas in the troposphere there may be a slight increase in spectral slope. Whether this relatively small effect (which would be eliminated with a factor of only 2–3 increase in the high wave number energy) is real, an artifact due to the commercial aircraft deviating to avoid storms [18] or a consequence of strong horizontal tropospheric anisotropy is still not clear. In contrast, in the vertical the empirical situation is much simpler since the largest relevant scales are 10–20 km which are experimentally accessible with balloons. From the 1960s onwards various studies [14–17] found Bogliano-Obhukov $k^{-11/5}$ scaling, supporting the anisotropic cascade picture.

 0031-9007/01/86(22)/5200(4)$15.00

From the empirical evidence of the $k^{-5/3}$ horizontal and $k^{-11/5}$ vertical scalings, an anisotropic cascade picture emerged, as well as a corresponding anisotropic "unified scaling" model [17,18] which combines both scalings and has an "in between" elliptical dimension = 23/9 [17].

A straightforward way of overcoming the relative paucity of large scale velocity data is to use remotely sensed cloud data. For example, a single cloud scene of 1000 pixels on a side has roughly the same information content as the entire GASP experiment. Clouds are strongly nonlinearly coupled with the velocity field, so that if the scale invariant symmetry is broken in the velocity field, it will almost certainly be broken in the cloud field (and vice versa). In addition, 2D cloud images have the advantage that unlike 1D aircraft data, they are largely unbiased by horizontal anisotropy.

We performed a direct check of the cascade model by using 909 satellite cloud pictures at both infrared and visible wavelengths, from three satellites and with a year of (near) daily data. The primary data set was obtained from the Atmospheric Radiation Measurement archives and consisted of scenes over their Oklahoma test site ("CART") from the sun-synchronous NOAA-12 and NOAA-14 satellites' Advanced Very High Resolution Radiometer (AVHRR) sensor with subscenes centered over Wichita, Kansas. In addition, a smaller set of geostationary GMS-5 images over the central Pacific were also used. The geostationary meteorological satellite (GMS) data were taken within a month of each other and so were less representative of the meteorological variability but had the advantage of extending the range of scales to over 5000 km (only the central 1024×1024 pixel square was used in order to minimize cartographic distortion). The sampling was reasonably complete and unbiased even though images were not received every day and some winter (visible) images were rejected due to insufficient light (see [27] for more details). Overall 284 visible and 564 IR AVHRR images were used (1.1 km resolution), as well as 29 visible, 29 IR GMS images (5 km resolution).

To understand the analysis, recall that cascades were originally developed to study intermittency in turbulent energy fluxes (ε) which are (on average) conserved from scale to scale during the cascade. Starting at a large outer scale, due to instability or nonlinear interactions, large structures break up into smaller eddies, the flux through the latter being multiplicatively modulated by the former. This process repeats scale after scale until it is finally stopped by the action of viscosity at small scales. The variability at scale ratio λ is

$$\langle \varepsilon_\lambda^q \rangle = \lambda^{K(q)}; \qquad \lambda = \frac{L_{\text{eff}}}{l}. \tag{1}$$

ε_λ is the energy flux nondimensionalized by the ensemble mean flux, L_{eff} is the effective outer scale of the cascade, l is the scale of an eddy, the angular brackets indicate statistical averaging, and $K(q)$ is a convex function which characterizes the multiscaling. This fundamental cascade equation describes the variability from the weak fluctuations (low q) up to strong fluctuations (high q) at all scales. When $l = L_{\text{eff}}$, we have $\lambda = 1$ and $\langle \varepsilon_1^q \rangle = 1$ implying that ε_1 is a "sure" (nonrandom) value; L_{eff} is therefore the outer scale of a pure cascade which would yield all the observed variability. Since the true cascade process has variable input flux at the largest scale, not all the variability is due to the cascade; hence if a true (infinite) ensemble were used to estimate the moments, L_{eff} would be an upper bound on the outer scale. At the small scales, due to the finite cloud thickness, the inner radiance scale could be larger than the viscous scale (see [28]).

In order to test the cascade hypothesis, it is sufficient to estimate a (scale by scale) conservative quantity analogous to the energy flux which we denote by φ and to systematically degrade its resolution (by averaging, "coarse graining," or equivalently by using wavelets) to obtain φ_λ. For each moment q, we can then perform a linear regression of $\log\langle \varphi_\lambda^q \rangle$ against $\log\lambda$ to test Eq. (1) (with φ instead of ε) and estimate $K(q)$ from the slope and L_{eff} from the intercept.

In turbulence, the Kolmogorov law relates ε_λ to the corresponding velocity shears Δv by the linear scaling law $\Delta v_\lambda = \varepsilon_\lambda^a \lambda^{-H}$ (with $a = H = \frac{1}{3}$). A similar ("Corssin-Obhukov") scaling law holds for (passive) scalar field; for the radiances we expect an analogous relation $\Delta I_\lambda = \varphi_\lambda^a \lambda^{-H}$. Since the linear λ^{-H} scaling can be modeled by a fractional integration (power law filter) of order H (the fractionally integrated flux model [19,29]), its effect can be removed by differentiation of order $>H$; Ref. [30] shows that it is sufficient to use the modulus of the finite difference gradient vector [31] which is a numerical approximation of an isotropic differentiation of order $H = 1$. Reference [27] shows that on an image by image basis H varies between 0.2 and 0.6 and that H is the only parameter that had significant scene to scene variability; it was the only one which was systematically different over land and ocean. Also, without loss of generality, we may take $a = 1$ [19].

The result of the data analysis is shown in Fig. 1. As predicted by the cascade model, the power law scaling lines for the different moments point quite accurately to the same outer scale L_{eff}. Using linear regression of the log(moment) against $\log\lambda$ and using the intercept to estimate L_{eff} for each q value, we obtain 19 900 ± 3900 km, 19 500 ± 6200 km (visible, NOAA 12, 14), 24 500 ± 13 700 km, 27 500 ± 11 200 km (IR, NOAA 12, 14); the errors are those of the seven values of q shown in Fig. 1. The overall mean for the four is L_{eff} = 22 850 ± 3300 km (i.e., an extrapolation by a factor of 22 850/280 = 82 in scale). The limited GMS-5 sampling leads to an underestimate of the ensemble variability so that the GMS-5 data have $L_{\text{eff}} \approx 6330 \pm 230$ km, 3500 ± 240 km (IR, visible, respectively), i.e., an overall mean 4920 ± 1420 km. Although this difference of factor $\lambda' = 22\,850/4920 = 4.6$ may seem large, it actually

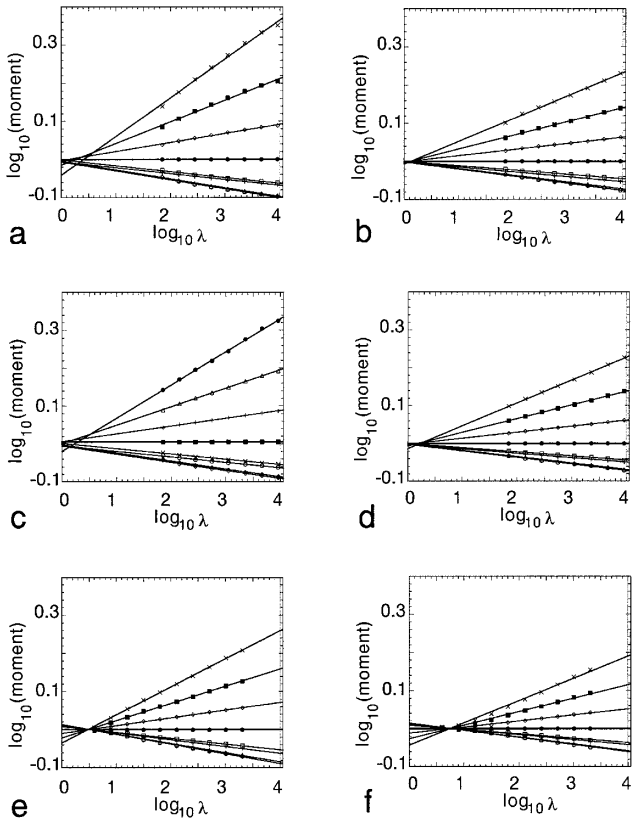

FIG. 1. The multiscaling of the moments ($\langle\varphi_\lambda^q\rangle$) as functions of scale ratio $\lambda = L_{\rm eff}/l$ for fields degraded to resolution l, and the effective outer scale $L_{\rm eff} = 20\,000$ km. (a) NOAA 12 infrared; (b) NOAA 12 visible; (c) NOAA 14 infrared; (d) NOAA 14 visible; (e) GMS-5 infrared; (f) GMS-5 visible.

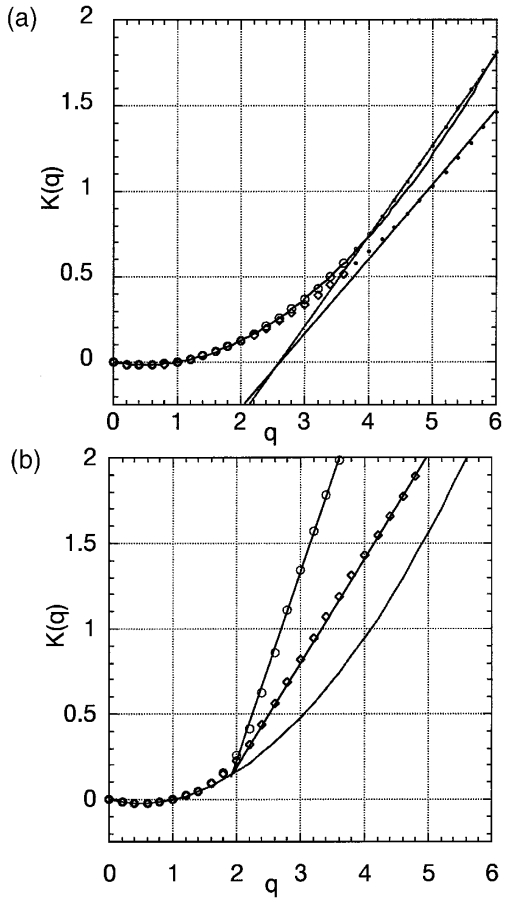

FIG. 2. (a) Visible: $K(q)$ against q; top points are for NOAA-12, bottom for NOAA 14, and the curve is the theory for $\alpha = 1.93$, $C_1 = 0.076$. The straight line asymptotes show second order multifractal phase transitions at $q_{\rm cr} = 3.8$, 4.2, respectively. (b) Infrared: $K(q)$ against q; top points are for NOAA-12, bottom for NOAA 14, and the curve is the theory for $\alpha = 1.94$, $C_1 = 0.083$. The straight line asymptotes show first order multifractal phase transitions at $q_{\rm cr} = 1.9$.

implies only a very small underestimate of the variability by the GMS-5 data: for example, using $K(2) = 0.16$ [Fig. 2(a)], we see that if the standard deviations were increased by a factor of only $(\lambda')^{K(2)/2} = 1.1$ then the two $L_{\rm eff}$ estimates would agree. Clearly some of this difference could be due to the different variabilities of clouds over land (AVHRR) compared to clouds over ocean (GMS). Note that the GMS data show that 4920 km is a lower bound on the true outer scale. Performing regressions with quadratic functions shows that the 2nd order terms are on average small: only 1.6%/octave in scale.

Finally, in Fig. 2, we compare the $K(q)$ functions estimated from the slopes in Fig. 1. We see that the visible and infrared data differ somewhat from each other; this is not surprising since the variability in the two are nonlinearly related, one depends on solar reflection, the other on blackbody emission. Note now that for both infrared and visible data, the $K(q)$ for the two satellites are nearly identical (and curved) until certain critical q values. For the visible data, they then seem to follow asymptotes tangent to the curves after critical values $q_{\rm cr} \approx 3.8$, $q_{\rm cr} \approx 4.2$ (NOAA 12, 14, respectively), whereas for the infrared data, they both seem to follow different nontangential asymptotes after $q_{\rm cr} \approx 1.9$. These are apparently the second and first order multifractal phase transitions described in [32,33]; the different asymptotic slopes are equal to the different maximum orders of singularities present in each sample. In second order phase transitions, $q_{\rm cr}$ is simply the largest that can reliably be estimated with the finite number of scenes; in first order transitions $q_{\rm cr}$ is due to the divergence of moments combined with the effect of finite sample size. Since the data sets do not have the same number of scenes, for $q > q_{\rm cr}$ the slopes are different, while for $q < q_{\rm cr}$, they are insensitive to sample size.

In order to make quantitative comparisons of the $K(q)$'s, we have fit the latter to the functional forms theoretically predicted on the basis of "universal multifractals" which are stable, attractive multifractal processes (for the debate, see [23]):

$$K(q) = \frac{C_1}{\alpha - 1}(q^\alpha - q), \qquad (2)$$

where C_1 is the codimension of the mean singularity and α is the Levy index which characterizes the degree of multifractality; Fig. 2 graphically shows the excellent fits which

are obtained up to the phase transitions. Although some variation between NOAA and GMS is expected since the former is mainly over land, while the latter is over ocean, if we take the average for each wavelength, we obtain $\alpha = 1.91 \pm 0.02$, $C_1 = 0.077 \pm 0.001$, (visible) $\alpha = 1.90 \pm 0.03$, $C_1 = 0.0845 \pm 0.004$ (infrared). These can be compared to values obtained from a recent study of 38 ground based visible cloud images over the scale range 1 m–1 km [28] which obtained (the similar) values $\alpha = 1.77$, $C_1 = 0.061$ (see also [34–36]).

Because of the *ad hoc* assumption of isotropic scaling, standard turbulence approaches have great difficulty explaining two basic empirical observations: (a) how the vertical and horizontal scalings can be so different from each other and (b) how the horizontal scaling can be respected so well right through the mesoscale. However, we have seen that anisotropic cascades starting at planetary scales can easily account for the observed variability in cloud radiance fields over the entire range 1–5000 km, for both weak and strong fluctuations/structures. Since such cascades generically give rise to multifractal fields with their hierarchies of strong structures (mathematically, singularities), this picture neatly accounts for the "coherent structures"; indeed, in the infrared we find evidence for particularly strong self-organized critical structures possibly related to thermal "fronts" in agreement with the earlier empirical evidence of dynamical self-organized structures [37]. Finally, since such anisotropic scaling generally leads to systematic changes in morphology with scale, this wide range scaling turns out to be compatible with standard meteorology.

We thank P. Minnett for supplying the ARM data and J. Duan, M. Larcheveque, E. Lindborg, F. Schmitt, I. Tchiguirinskaia, and A. Tuck for valuable discussions. D. S. acknowledges the hospitality of the Mathematical Sciences Department of Clemson University.

[1] L. F. Richardson, *Weather Prediction by Numerical Process* (Cambridge University Press, Cambridge, United Kingdom, 1922, republished by Dover, New York, 1965).
[2] A. N. Kolmogorov, Proc. Acad. Sci. USSR, Geochem. Sect. **30**, 299–303 (1941).
[3] R. Fjortoft, Tellus **7**, 168–176 (1953).
[4] R. H. Kraichnan, Phys. Fluids **10**, 1417–1423 (1967).
[5] H. A. Panofsky and I. Van der Hoven, Q. J. R. Meteorol. Soc. **81**, 603 (1955).
[6] I. Van der Hoven, J. Meteorol. **14**, 160–164 (1957).
[7] J. L. Goldman, "The Power Spectrum in the Atmosphere below Macroscale," Institute of Desert Research, University of St. Thomas, Houston, TX, 1968.
[8] N. Z. Pinus, E. R. Reiter, G. N. Shur, and N. K. Vinnichenko, Tellus **19**, 206–213 (1967).
[9] A. S. Monin, *Weather Forecasting as a Problem in Physics* (MIT Press, Boston, MA, 1972).
[10] G. D. Nastrom and K. S. Gage, Tellus **35**, 383 (1983).
[11] G. D. Nastrom, K. S. Gage, and W. H. Jasperson, Nature (London) **310**, 36–38 (1984).
[12] S. Lovejoy, Science **187**, 1035–1037 (1982).
[13] D. Schertzer and S. Lovejoy, Phys.-Chem. Hydrodyn. J. **6**, 623–635 (1985).
[14] R. M. Endlich, R. C. Singleton, and J. W. Kaufman, J. Atmos. Sci. **26**, 1030–1041 (1969).
[15] S. I. Adelfang, J. Atmos. Sci. **10**, 138 (1971).
[16] A. Lazarev, D. Schertzer, S. Lovejoy, and Y. Chigirinskaya, Nonlinear Processes Geophys. **1**, 115–123 (1994).
[17] D. Schertzer and S. Lovejoy, in *Turbulent Shear Flow,* edited by B. Launder (Springer-Verlag, Berlin, 1985), Vol. 4, pp. 7–33.
[18] S. Lovejoy, D. Schertzer, P. Silas, Y. Tessier, and D. Lavallée, Ann. Geophys. **11**, 119–127 (1993).
[19] D. Schertzer, S. Lovejoy, F. Schmitt, Y. Chigirinskaya, and D. Marsan, Fractals **5**, 427–471 (1997).
[20] S. Lovejoy *et al.,* J. Plankton Res. **23**, 117–141 (2001).
[21] C. Meneveau and K. R. Sreenivasan, Phys. Lett. A **137**, 103–112 (1989).
[22] F. Schmitt, D. Lavallée, D. Schertzer, and S. Lovejoy, Phys. Rev. Lett. **68**, 305 (1992).
[23] D. Schertzer and S. Lovejoy, J. Appl. Meteorol. **36**, 1296–1303 (1997).
[24] E. Lindborg, J. Fluid Mech. **388**, 259–288 (1999).
[25] J. Courbage, S. Lovejoy, H. Gaoanac'h, and D. Schertzer, EOS Trans. Am. Geophys. Union **81**, F576 (2000).
[26] A. F. Tuck and S. J. Hovde, Geophys. Res. Abstracts **1**, 772 (1999).
[27] J. D. Stanway, M.Sc. Thesis, McGill University, 2000.
[28] D. Sachs, S. Lovejoy, and D. Schertzer, Fractals (to be published).
[29] D. Schertzer and S. Lovejoy, J. Geophys. Res. **92**, 9693–9714 (1987).
[30] D. Lavallée, S. Lovejoy, D. Schertzer, and P. Ladoy, in *Fractals in Geography,* edited by L. De Cola and N. Lam (Prentice-Hall, Englewood Cliffs, NJ, 1993), pp. 171–205.
[31] $\varphi = \sqrt{[I'(x+1,y) - I'(x,y)]^2 + [I'(x,y+1) - I'(x,y)]^2}$ where x, y are in units of pixels. The only remaining technicality arises from the insufficient dynamical range of the images. Although they nominally had 10 bits/pixel, most images actually had ranges of less than 200 digital counts (i.e., 7–8 bits/pixel). This resulted in many spurious zero gradient regions (neighboring pixels with nominally the same digital value). To alleviate this problem (which affects the weak gradient dominated low q statistics), an initial fractional integration of order $H_s = 0.2$ was used; this is a scale invariant smoothing [i.e., convolution $I'(r) = I(r)^* |r|^{-(D-H_s)}$ with $D = 2$]. Since the result is a 32 bit field, the spurious zero gradients are effectively eliminated.
[32] D. Schertzer and S. Lovejoy, Physica (Amsterdam) **185A**, 187–194 (1992).
[33] D. Schertzer and S. Lovejoy, in *Fractals in the Natural and Applied Sciences,* edited by M. Novak (Elsevier, North-Holland, Amsterdam, 1994), pp. 325–339.
[34] Y. Tessier, S. Lovejoy, and D. Schertzer, J. Appl. Meteorol. **32**, 223–250 (1993).
[35] A. Arneodo, N. Decoster, and S. G. Roux, Phys. Rev. Lett. **83**, 12 155 (1999).
[36] A. P. Siebsesma and H. J. J. Jonker, Phys. Rev. Lett. **85**, 214 (2000).
[37] Y. Chigirinskaya, D. Schertzer, S. Lovejoy, A. Lazarev, and A. Ordanovich, Nonlinear Proc. Geophys. **1**, 105–114 (1994).